J Cardiovasc Imaging. 2022 Oct;30(4):292-304
https://doi.org/10.4250/jcvi.2021.0141
pISSN 2586-7210·eISSN 2586-7296

Journal of Cardiovascular Imaging JCVI

Original Article

Distribution of Aortic Root Calcium in Relation to Frame Expansion and Paravalvular Leakage After Transcatheter Aortic Valve Implantation (TAVI): An Observational Study Using a Patient-specific Contrast Attenuation Coefficient for Calcium Definition and Independent Core Lab Analysis of Paravalvular Leakage

Nahid El Faquir, MD[1], Quinten Wolff, BSc[1], Rafi Sakhi, MD[1], Ben Ren, MD, PhD[1,2], Zouhair Rahhab, MD[1], Sander van Weenen, BSc[1], Patrick Geeve, BN[1], Ricardo P J Budde, MD, PhD[3], Eric Boersma, PhD[1], Joost Daemen, MD, PhD[1], Nicolas M van Mieghem, MD, PhD[1], and Peter P de Jaegere, MD, PhD[1]

[1]Department of Cardiology, Thoraxcenter, Erasmus Medical Center, Rotterdam, The Netherlands
[2]Cardialysis Clinical Trials Management and Core Laboratories, Rotterdam, The Netherlands
[3]Department of Radiology and Nuclear Medicine, Erasmus Medical Center, Rotterdam, The Netherlands

Received: Aug 26, 2021
Revised: Feb 24, 2022
Accepted: May 15, 2022
Published online: Jul 1, 2022

Address for Correspondence:
Peter P de Jaegere, MD, PhD
Department of Cardiology, Thoraxcenter, Erasmus Medical Center, Doctor Molewaterplein 40, 3015 GD Rotterdam, The Netherlands.
Email: p.dejaegere@erasmusmc.nl

ORCID iDs
Nahid El Faquir
https://orcid.org/0000-0001-6718-5511
Quinten Wolff
https://orcid.org/0000-0002-8664-7758
Rafi Sakhi
https://orcid.org/0000-0002-4699-9011
Zouhair Rahhab
https://orcid.org/0000-0002-1787-5749
Ricardo P J Budde
https://orcid.org/0000-0003-3792-615X
Eric Boersma
https://orcid.org/0000-0002-2559-7128
Joost Daemen
https://orcid.org/0000-0001-8628-1410
Nicolas M van Mieghem
https://orcid.org/0000-0002-2732-1205

ABSTRACT

BACKGROUND: Calcium is a determinant of paravalvular leakage (PVL) after transcatheter aortic valve implantation (TAVI). This is based on a fixed contrast attenuation value while X-ray attenuation is patient-dependent and without considering frame expansion and PVL location. We examined the role of calcium in (site-specific) PVL after TAVI using a patient-specific contrast attenuation coefficient combined with frame expansion.
METHODS: 57 patients were included with baseline CT, post-TAVI transthoracic echocardiography and rotational angiography (R-angio). Calcium load was assessed using a patient-specific contrast attenuation coefficient. Baseline CT and post-TAVI R-angio were fused to assess frame expansion. PVL was assessed by a core lab.
RESULTS: Overall, the highest calcium load was at the non-coronary-cusp-region (NCR, 436 mm^3) vs. the right-coronary-cusp-region (RCR, 233 mm^3) and the left-coronary-cusp-region (LCR, 244 mm^3), $p < 0.001$. Calcium load was higher in patients with vs. without PVL (1,137 vs. 742 mm^3, $p = 0.012$) and was an independent predictor of PVL (odds ratio, 4.83, $p = 0.004$). PVL was seen most often in the LCR (39% vs. 21% [RCR] and 19% [NCR]). The degree of frame expansion was 71% at the NCR, 70% at the RCR and 74% at the LCR without difference between patients with or without PVL.
CONCLUSIONS: Calcium load was higher in patients with PVL and was an independent predictor of PVL. While calcium was predominantly seen at the NCR, PVL was most often at

Journal of Cardiovascular Imaging JCVI

Peter P de Jaegere
https://orcid.org/0000-0003-1540-0755

Funding

Dr. Daemen received institutional grant/research support from Astra Zeneca, Abbott Vascular, Boston Scientific, ACIST Medical, Medtronic, Pie Medical, and ReCor Medical, and consultancy and speaker fees from ACIST Medical, Boston Scientific, ReCor Medical, Pie Medical and Medtronic. Prof. Van Mieghem reports grants from Abbott, grants from Boston Scientific, grants from Edwards Lifesciences, grants from Medtronic, grants from Daiichi Sankyo, grants from PulseCath BV and grants from Teleflex, outside the submitted work. Dr. Wolff reports non-financial support from Siemens Healthcare, during the conduct of the study.

Conflict of Interest

The authors have no financial conflicts of interest.

Author Contributions

Conceptualization: El Faquir N, Wolff Q, Sakhi R, Ren B, Rahhab Z, Van Weenen S, Geeve P, Budde RPJ, Boersma E, Daemen J, Van Mieghem NM, De Jaegere PP; Data curation: El Faquir N, Wolff Q, Sakhi R, Ren B, Rahhab Z, Van Weenen S, Geeve P, Budde RPJ, Van Mieghem NM, De Jaegere PP; Formal analysis: El Faquir N, Sakhi R, Ren B, Rahhab Z, Boersma E, De Jaegere PP; Investigation: El Faquir N, Wolff Q, Sakhi R, Ren B, Rahhab Z, Van Weenen S, Geeve P, Budde RPJ, Boersma E, Daemen J, Van Mieghem NM, De Jaegere PP; Methodology: El Faquir N, Wolff Q, Sakhi R, Ren B, Rahhab Z, Van Weenen S, Geeve P, Budde RPJ, Boersma E, Daemen J, Van Mieghem NM, De Jaegere PP; Project administration: El Faquir N, Wolff Q, Sakhi R, Ren B, Rahhab Z, Van Weenen S, Geeve P, Budde RPJ, Boersma E, Van Mieghem NM, De Jaegere PP; Resources: El Faquir N, Wolff Q, Sakhi R, Ren B, Rahhab Z, Van Weenen S, Geeve P, Budde RPJ, Van Mieghem NM, De Jaegere PP; Software: El Faquir N, Wolff Q, Sakhi R, Ren B, Van Weenen S, Geeve P, Budde RPJ, Van Mieghem NM, De Jaegere PP; Supervision: El Faquir N, Ren B, Rahhab Z, Van Weenen S, Geeve P, Budde RPJ, Boersma E, Daemen J, Van Mieghem NM, De Jaegere PP; Validation: El Faquir N, Wolff Q, Sakhi R, Ren B, Rahhab Z, Van Weenen S, Geeve P, Budde RPJ, Boersma E, Daemen J, Van Mieghem NM, De Jaegere PP; Visualization: El Faquir N, Wolff Q, Sakhi R, Ren B, Rahhab Z, Van

the LCR. These findings indicate that in addition to calcium, specific anatomic features play a role in PVL after TAVI.

Keywords: Aortic stenosis; Transcatheter aortic valve replacement; Multimodal imaging

INTRODUCTION

Outcome of transcatheter aortic valve implantation (TAVI) has continuously improved over the last decade and is currently approved by the FDA for the treatment of low risk patients.[1-5] Notwithstanding improvements in operator experience and valve technology, paravalvular leakage (PVL) may still occur and is seen more often after TAVI than after surgical aortic valve replacement (SAVR).[4-13] It is associated with impaired survival in certain patient categories and, conceptually, may be more of a concern in low risk patients as they have a longer projected longevity.[6]

Different patient- and procedure related factors such as among others calcium, sizing and depth of implantation have been identified as determinants of PVL.[9][13][14] With respect to calcium—that at variance with SAVR is not removed during TAVI—all studies assessing the role of calcium and PVL have been based upon a fixed software defined value of attenuation of the incoming X-rays for the differentiation between calcium and non-calcified tissue while X-ray attenuation is a patient-dependent phenomenon.[14-16] In addition, PVL is the result of a device-host interaction that is specific for each individual patient. The objective of this study was to further elucidate the role of calcium and its distribution within the aortic root in the occurrence of PVL using a patient-specific contrast attenuation coefficient and fusion imaging (i.e., integration of frame expansion [rotational angiography {R-angio} immediately after TAVI] with the patient's baseline anatomy [computed tomography {CT} before TAVI]).

METHODS

Patient population

The index population consisted of 134 patients with severe degenerative tricuspid aortic stenosis who underwent TAVI between July 2009 and September 2014 and in whom pre procedural multislice CT (MSCT), R-angio immediately after TAVI and pre discharge transthoracic echocardiography (TTE) were available. Patients with poor image quality (MSCT [n = 3], R-angio [n = 14], TTE [n = 32], fusion imaging [n = 28]) were excluded from analysis. The total population of the present study, therefore, consists of 57 patients. All patients gave written informed consent for anonymized prospective data collection for clinical research purpose (EMC Institutional Review Board: TAVI Care & Cure project, MEC-2014-277).

MSCT-baseline: calcium load and distribution

Dual source (Somatom Definition FLASH, Drive or Force; Siemens Healthcare GmbH, Forchheim, Germany) CT was used for sizing as previously described.[17] For the assessment of the calcium load, a contrast-enhanced prospectively electrocardiogram-triggered with a tube voltage of 120 kV, a reference tube current of 190 mAs at 30–50% of the ECR-R interval was used. Images were reconstructed at a 0.75 mm slice thickness with Bv40 kernel.[17] Measurements were acquired by performing planimetry on MSCT aided by 3Mensio software (Pie Medical Imaging BV, Maastricht, The Netherlands).[17]

https://doi.org/10.4250/jcvi.2021.0141

Journal of Cardiovascular Imaging JCVI

Weenen S, Geeve P, Budde RPJ, Van Mieghem NM, De Jaegere PP; Writing - original draft: El Faquir N, Wolff Q, Sakhi R, Ren B, Rahhab Z, Van Weenen S, Geeve P, Budde RPJ, Boersma E, Van Mieghem NM, De Jaegere PP; Writing - review & editing: El Faquir N, Wolff Q, Sakhi R, Ren B, Rahhab Z, Van Weenen S, Geeve P, Budde RPJ, Boersma E, Daemen J, Van Mieghem NM, De Jaegere PP.

After automatic reconstruction and segmentation of the aortic root, the aortic annulus was manually defined as a virtual plane containing the basal attachment point of the 3 aortic valve leaflets. Subsequently, the software automatically created a multiplanar reconstruction of the aortic root in short- and long-axis view perpendicular to the manually preferable defined centerline. The window of interest was defined into 3 specific area's (**Figure 1A and B**): (1) The supra-annular area (SAA) was defined from the annular plane till the ostium of the first coronary artery that branches off the ascending aorta; (2) Left ventricular outflow tract (LVOT) was defined from 6 mm below the annular plane till the annular plane; (3) Total aortic root was defined as the sum of both areas (SAA + LVOT: total area). The software automatically subdivided each area into 3 specific regions according to the 3 coronary cusp regions (non coronary cusp region [NCR], right coronary cusp region [RCR] and left coronary cusp region [LCR]). Concerning the asymmetric distribution of calcium per area, the software provided visual short- and long-axis views of the calcium distribution (**Figure 1A-C**). All measurements were performed in the systolic phase (at 30–50% of R wave).

Given the variability in intraluminal contrast attenuation between patients, a patient-specific calcium detection threshold was used similar to the method of Hansson et al.[18] For that purpose, a polygonal surface in a homogeneous blood pool region 10 mm above the ostium of the first coronary that branches of was selected (**Figure 1D**) from which a mean attenuation value and the standard deviation was calculated. The patient-specific attenuation threshold was defined using the following formula: Calcium Detection Threshold/Mean Attenuation Value + 4 Standard Deviation (SD) Attenuation Value. Any level above this threshold was used to define the amount of calcium for each individual patient and was expressed by mm^3. The amount of calcium (i.e., calcium load) was calculated for the entire aortic root (SAA + LVOT), the area above the annulus up to the level of the coronary ostia (SAA), the area below the

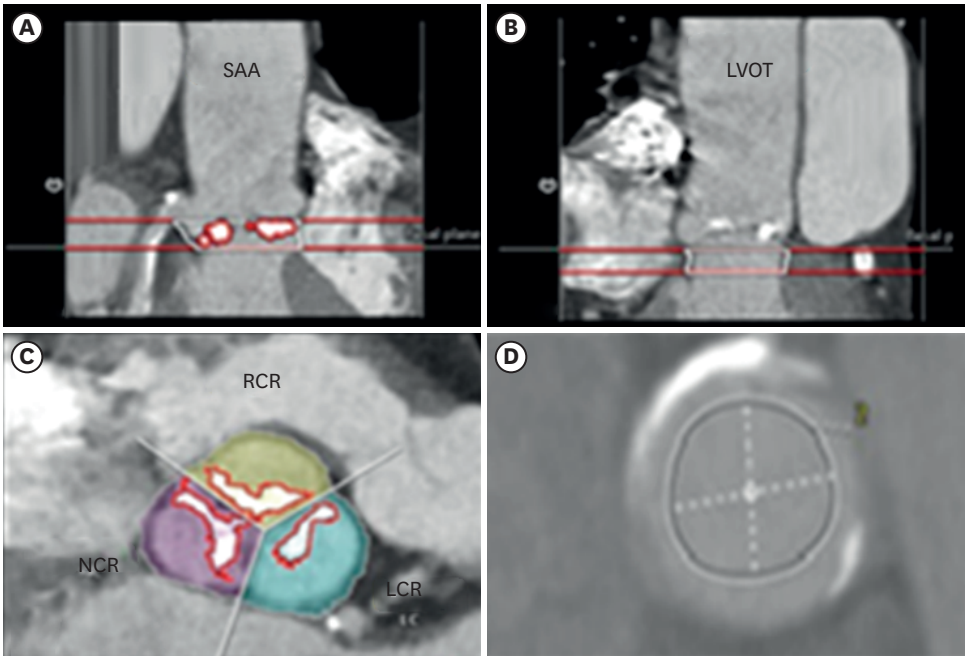

Figure 1. Multislice computed tomography aortic root dimensions. Multiplanar reconstruction views demonstrating the areas of interest. (A) SAA; (B) LVOT; (C) NCR, RCR and LCR; (D) Homogenous blood pool surface 10 mm above the ostium of the first coronary that branches of.
LCR: left coronary cusp region, LVOT: left ventricular outflow tract, NCR: non coronary cusp region, RCR: right coronary cusp region, SAA: supra-annular area.

https://doi.org/10.4250/jcvi.2021.0141

Journal of Cardiovascular Imaging JCVI

aortic annulus up to 6 mm below the annular plane (LVOT) and for the 3 different cusp areas (NCR, RCR, and LCR).

Intra- and interobserver variability of calcium load

All images were analysed by an experienced investigator after specific training (Sakhi R). A randomly selected sample of 30 patients of the index population was re-evaluated within 30 days to determine the intra-observer variability. A second experienced investigator (van Weenen S) blinded to the results of observer 1, analysed the same 30 patients for inter-observer variability assessment. The intraclass correlation coefficient (ICC) was satisfactory for all the measurements (ICC > 0.90) (**Supplementary Table 1**).

R-angio and fusion imaging: valve position and frame geometry in relation to aortic annulus

R-angio was performed immediately after TAVI by the Artis zee biplane angiographic C-arm system using dedicated software for motion compensation to reconstruct the valve frame (Siemens Healthcare GmbH) as described before.[8)9)19)20)] The image of the valve frame was fused with the preprocedural CT using the Siemens prototype software (Siemens Healthcare GmbH). First, the CT image was rotated until the projection angle did correspond with the one that was used during the TAVI procedure (**Figure 2A**). Next, the reconstructed valve frame was positioned into the aortic root derived from the baseline CT while respecting the orientation of the valve frame in the aortic root and the depth of implantation (i.e., distance inflow valve frame at the non coronary cusp [NCC] and left coronary cusp [LCC] to aortic annulus) (**Figure 2G**). The following measurements were performed in the cross-sectional view at the level of the annulus for each cusp: the distance between the center of the annulus and outer border of the baseline anatomy (i.e., longest distance) (**Figure 2E**) and the distance between the center of the annulus and the edge of the valve frame (i.e., shortest distance) (**Figure 2H**). The degree of expansion of the valve frame was assessed at the level of each cusp and was calculated by Shortest Distance/Longest Distance × 100.

PVL assessment

TTE was performed before hospital discharge using the Philips iE33 ultrasound system (Philips Medical System, Best, The Netherlands) according to a standard acquisition protocol. Color Doppler recordings were optimized for display with the color velocity scale at 59.3 cm/s (50–70 cm/s). All echocardiograms were analysed by a core laboratory using the Image Arena workstation (TomTec Imaging System, Unterschleissheim, Germany). The analysts were blinded to patient- and procedure-related information except patient's height and weight.[21)]

The presence, location and severity of aortic regurgitation were assessed according to the Valve Academic Research Consortium (VARC)-2 criteria and expert opinions.[21)22)] PVL location and severity was assessed in the parasternal short-axis (PSAX) view in which the location was assigned to 12 locations based on a clock face and the severity was solely assessed based on the circumferential extent of PVL. Only mosaic color reflecting turbulent flow high velocity PVL jet(s) were measured (**Supplementary Figure 1**). In case of negative PSAX view finding, PVL was further assessed in the parasternal long-axis, apical 5-chamber and apical 3-chamber views, in which the PVL location was assigned as anterior or posterior to the prosthesis and the jet neck width (perpendicular to the flow) was measured and used in this study as an outcome measure. If multiple jets were seen in the same anatomic coronary cusp region, the measure of each jet was summed.

https://doi.org/10.4250/jcvi.2021.0141

Journal of Cardiovascular Imaging JCVI

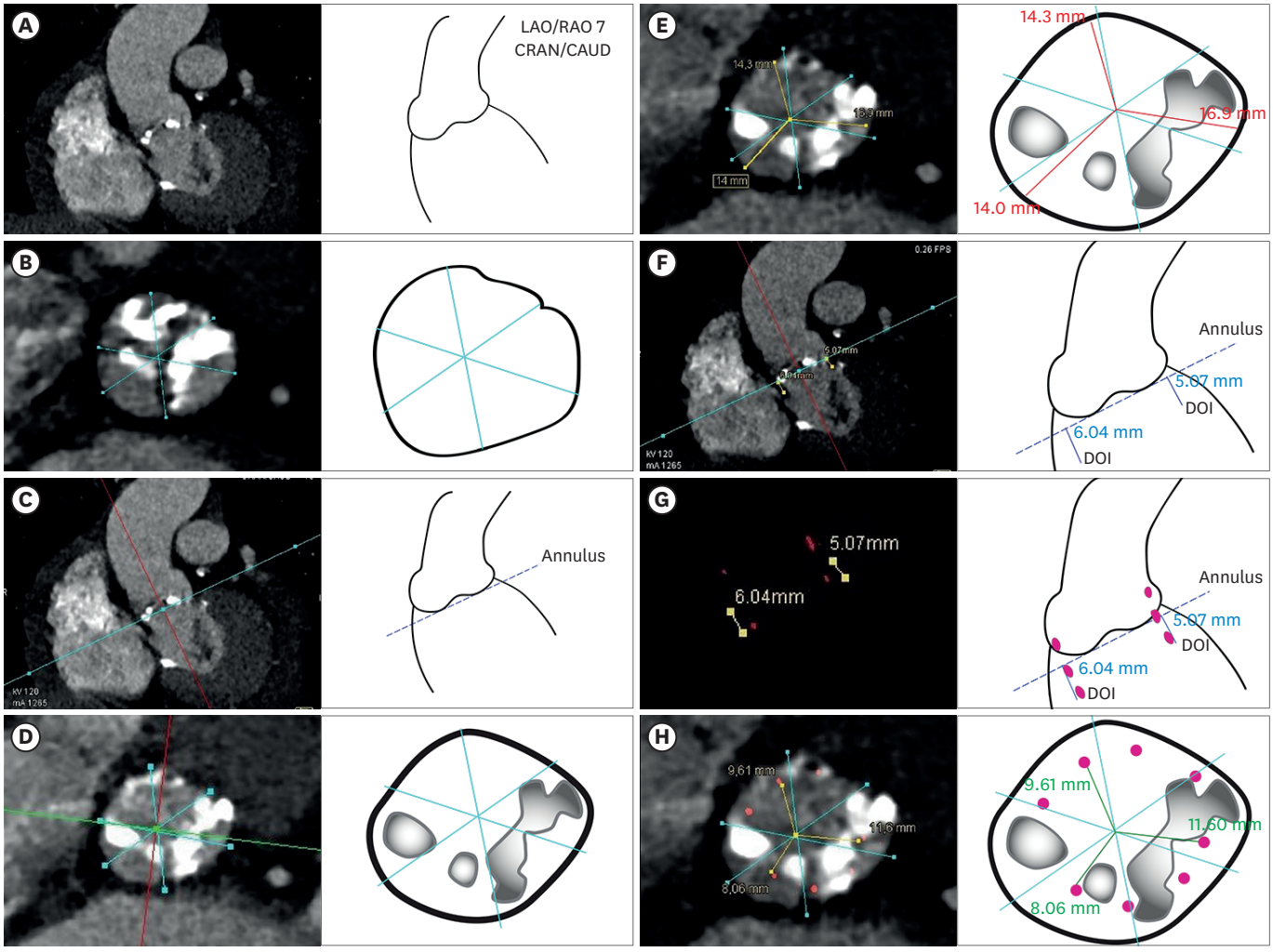

Figure 2. Workflow of fusion of pre-procedural CT and post-procedural R-angio. (A) Frontal view of the aorta and left ventricular outflow tract corresponding with the angulation of X-ray gantry used during implantation (in this case LAO 7/CRAN 10). (B) Cross sectional view of the sinus of Valsalva that was used for the definition of the center-point of the aortic root (i.e., the crossing of the 3 light blue lines starting from the middle portion of each cusp). (C) Frontal view of the aortic annulus. (D) Cross sectional view of the aortic annulus (C) with superposition of the light blue lines defining the center-point (B). (E) Cross sectional view of the aortic annulus with the measurement of the distance from the center-point to the outer border of the aortic annulus for each cusp (red lines). (F) Frontal view of the aortic annulus with depth of implantation of the valve-frame at the NCC and LCC in accordance to the actual depth of implantation measured on the angiogram after implantation (blue lines). (G) Frontal view of the aortic annulus with the fusion of the CT and R-angio, showing the superposition of the valve derived from the R-angio (red points) on the baseline CT respecting the actual depth of implantation and angle of X-ray gantry used during implantation. (H) Cross sectional view of the aortic annulus with the measurement of the distance from the center-point to the edge of the valve frame (red points) for each cusp (green lines).
CAUD: caudal, CRAN: cranial, CT: computed tomography, DOI: depth of implantation, LAO: left anterior oblique, LCC: left coronary cusp, NCC: non coronary cusp, R-angio: rotational angiography, RAO: right anterior oblique.

Statistical analysis

Normality of distributions was assessed by the Shapiro-Wilk test. Subsequently continuous variables were presented as mean ± SD or median (interquartile range). Categorical variables are expressed as frequencies and percentages. Baseline patient characteristics, including calcium load, procedural characteristics and fusion imaging variables were compared between patients with or without PVL by means of the Student's t-test, Mann-Whitney U test (continuous data) or χ^2 test (categorical data). Spearman-Rho correlation coefficients were used to assess the relation between (1) calcium load & degree of frame expansion and (2) degree of frame expansion & PVL jet width. Logistic regression analyses were performed to study calcium load and frame expansion as determinants of PVL. We considered site (NCR,

https://doi.org/10.4250/jcvi.2021.0141

Journal of Cardiovascular Imaging JCVI

RCR, LCR) and not patient, as unit of analysis. Model parameters were therefore estimated by generalized estimating equations to account for clustering of data within a patient. We also ran models that included 'site' × 'calcium load' and 'site' × 'frame expansion' interaction terms (with 'site' modelled by 2 dummy variables) to study if the relation between calcium load and frame expansion vs. PVL was modified by site (i.e., if that relation was site-specific) which was not the case. Statistical significance was assumed when the p-value was < 0.05. Statistical analysis was done using SPSS 24.0 (IBM Corporation, New York, NY, USA).

RESULTS

The baseline and procedural characteristics of the study population including the presence and severity of PVL before discharge are summarised in **Tables 1** and **2**. Any degree of PVL was observed in 34 out of the 57 patients (60%) (**Figure 3**). There was a similar distribution of the use of predilatation before TAVI and valve technology between patients with and without PVL. In comparison with patients without PVL, those with PVL had a higher calcium load (predominantly in the SAA) and 12 (35%) underwent post-dilation (**Figure 3**). Valve frame expansion and depth of implantation did not differ. The distribution of calcium is shown in **Figure 4**. Most if not all was seen in the SAA in the NCR.

PVL, calcium load and distribution relationships

PVL was observed most frequently in the LCR area (39%), followed by the RCR (21%) and NCR (19%) (**Figure 3**). The odds PVL at LCR was 2.63 (95% confidence interval, 1.12–6.19) (**Table 3**).

The calcium load at the total area and SAA were independent predictors for the presence of PVL (**Table 3**).

Fusion imaging

There was no difference in degree of frame expansion between patients with or without PVL (**Table 2**). There was also no significant correlation between the calcium load and degree of frame expansion (**Figure 5A**). No correlation was seen between PVL jet width and degree of frame expansion in patients with PVL except at the NCR (R= −0.39, p = 0.024) (**Figure 5B**).

DISCUSSION

The main findings of the present study are that aortic root calcium is predominantly located at the NCR in patients with and without PVL. Patients with PVL had a significantly larger amount of calcium compared to those without. Despite the fact that most calcium was at the NCR, the site of PVL was most often at the LCR. Except for calcium there were no other patient-, procedure- and/or device-related factors independently associated with PVL. Interestingly, balloon dilatation post TAVI was more often performed in patients with PVL. The aggregate of the findings indicates that in addition to calcium, specific anatomic features play a role in the occurrence of PVL after TAVI.

They need, however, to be interpreted in the context of the small scale and single-centre nature of the study of which the objective was to assess the relationship between calcium load and distribution and PVL. This is the reason why distinction was made between patients

https://doi.org/10.4250/jcvi.2021.0141

Journal of Cardiovascular Imaging JCVI

Table 1. Baseline characteristics including calcium load and distribution

Characteristics	Total population (n = 57)	No PVL (n = 23)	PVL (n = 34)	p-value
Demographics				
Age (year)	80 (74–85)	81 (75–85)	79 (72–84)	0.420
Male	30 (53)	11 (48)	19 (56)	0.550
Height (cm)	168 ± 9	168 ± 10	168 ± 8	0.890
Weight (kg)	75 ± 14	78 ± 13	73 ± 14	0.180
Body mass index (kg/m^2)	26 (23–29)	27 (24–32)	26 (22–28)	0.200
Cardiac risk factors				
Diabetes mellitus	14 (25)	9 (39)	5 (15)	0.036
Hypertension	46 (81)	20 (87)	26 (77)	0.500
Medical history				
Previous cerebrovascular event	13 (23)	5 (22)	8 (24)	0.870
Previous myocardial infarction	13 (23)	8 (35)	5 (15)	0.076
Previous coronary artery bypass graft surgery	13 (23)	7 (30)	6 (18)	0.260
Previous percutaneous coronary intervention	15 (26)	5 (22)	10 (29)	0.520
Peripheral vascular disease	15 (26)	9 (39)	6 (18)	0.071
Pulmonary hypertension	4 (7)	3 (13)	1 (3)	0.290
Chronic obstructive pulmonary disease	9 (16)	4 (17)	5 (15)	
Atrial fibrillation	18 (32)	7 (30)	11 (32)	
Permanent pacemaker	1 (2)	0	1 (3)	
NYHA class ≥ III	46 (81)	21 (91)	25 (74)	0.170
Laboratory				
Creatinine (umol/L)	92 (73–121)	92 (80–127)	89 (72–120)	0.340
Hemoglobin (g/dL)	7.8 ± 1.0	7.6 ± 0.9	8.0 ± 1.0	0.110
Risk score				
Logistic euroscore	12 (7–20)	16 (10–24)	10 (6–14)	0.016
Multi-sliced computed tomography				
Annulus				
Minimal diameter (mm)	22 ± 2	22 ± 2	22 ± 2	0.510
Maximal diameter (mm)	27 ± 2	27 ± 3	27 ± 2	0.860
Mean diameter (mm)	25 ± 2	24 ± 2	25 ± 2	0.710
Perimeter derived diameter (mm)	25 ± 2	25 ± 2	25 ± 2	0.840
Area derived diameter (mm)	24 ± 2	24 ± 2	24 ± 2	0.900
Perimeter (mm)	77 ± 6	77 ± 7	78 ± 6	0.850
Area (mm^2)	468 ± 74	465 ± 83	471 ± 68	0.760
LVOT				
Perimeter derived diameter (mm)	24 ± 2	24 ± 3	24 ± 2	0.690
Area derived diameter (mm)	24 ± 2	24 ± 3	24 ± 2	0.660
Perimeter (mm)	76 ± 7	77 ± 9	76 ± 6	0.630
Area (mm^2)	441 ± 89	451 ± 106	436 ± 76	0.530
Calcium load (mm^3)				
Aortic root	976 (543–1,371)	742 (354–1,251)	1,137 (697–1,598)	0.012
Non coronary region	436 (256–692)	305 (159–624)	559 (385–722)	0.015
Right coronary region	233 (115–380)	159 (64–268)	248 (168–478)	0.019
Left coronary region	244 (130–414)	156 (103–395)	283 (163–453)	0.029
Supra-annular area	862 (534–1,326)	702 (354–1,239)	1,114 (677–1,521)	0.008
Non coronary region	413 (256–628)	302 (159–511)	514 (364–659)	0.011
Right coronary region	227 (115–379)	159 (64–266)	244 (167–477)	0.019
Left coronary region	235 (127–377)	153 (103–316)	253 (155–436)	0.018
LVOT	6 (1–75)	1 (0–65)	11 (2–81)	0.095
Non coronary region	1 (0–21)	1 (0–9)	2 (0–23)	0.340
Right coronary region	0 (0–1)	0 (0–1)	1 (0–2)	0.300
Left coronary region	1 (0–21)	0 (0–5)	3 (0–30)	0.200

Values are expressed in median (interquartile range), number (%) or mean ± standard deviation.
PVL: paravalvular leakage, NYHA: New York Heart Association functional classification, LVOT: left ventricular outflow tract.

without and those with any degree of PVL, prognosis was not the objective. Sample size and single-centre nature may have impeded to elucidate (patient/procedure-related) factors other than calcium to be associated with PVL. This also holds for valve type. There was an

https://doi.org/10.4250/jcvi.2021.0141

Journal of Cardiovascular Imaging JCVI

Table 2. Procedural characteristics and technical outcome

Characteristics	Total population (n = 57)	No PVL (n = 23)	PVL (n = 34)	p-value
Transfemoral access	55 (97)	22 (96)	33 (97)	
Pre balloon dilatation	49 (86)	19 (83)	30 (88)	0.700
Valve type				
Self-expandable	32 (56)	12 (52)	20 (59)	0.620
Medtronic Corevalve	29 (51)	12 (52)	17 (50)	
St. Jude Portico	3 (5)	0	3 (9)	
Balloon-expandable	22 (39)	8 (35)	14 (41)	0.630
Edwards Sapien XT	11 (19)	3 (13)	8 (24)	
Edwards Sapien 3	9 (16)	5 (22)	4 (12)	
Mechanically expandable	3 (5)	3 (13)	0	0.061
Boston Lotus	3 (5)	3 (13)	0	
Valve size				
23	6 (11)	2 (9)	4 (12)	0.530
25	2 (4)	0	2 (6)	0.510
26	19 (33)	9 (39)	10 (29)	0.570
27	1 (2)	1 (4)	0	0.400
29	27 (47)	11 (48)	16 (47)	0.960
31	2 (4)	0	2 (6)	0.510
Post balloon dilatation	12 (21)	0	12 (35)	0.001
Depth of implantation non coronary cusp (mm)	7 (4–8)	5 (4–8)	7 (4–9)	0.350
Depth of implantation left coronary cusp (mm)	7 (4–8)	7 (4–8)	6 (4–9)	0.760
Fusion				
Degree of frame expansion (%)				
Annulus				
NCR	71 (63–76)	68 (63–75)	71 (63–77)	0.580
RCR	70 (61–82)	70 (62–83)	71 (60–81)	0.790
LCR	74 (66–81)	74 (69–85)	74 (63–81)	0.320
Pre discharge echocardiography				
PVL severity according to VARC-2 [21]				-
None	23 (40)	23 (100)	-	
Trace	4 (7)	-	4 (12)	
Mild	29 (51)	-	29 (85)	
Moderate	0	-	0	
Severe	1 (2)	-	1 (3)	
PVL severity according to expert opinion [22]				-
None	23 (40)	23 (100)	-	
Trace	4 (7)	-	4 (12)	
Mild	18 (32)	-	18 (53)	
Mild to Moderate	11 (19)	-	11 (32)	
Moderate	0	-	0	
Moderate to Severe	0	-	0	
Severe	1 (2)	-	1 (3)	

Values are expressed in number (%) or median (interquartile range).
PVL: paravalvular leakage, NCR: non coronary cusp region, RCR: right coronary cusp region, LCR: left coronary cusp region, VARC: Valve Academic Research Consortium.

equal distribution between balloon- and self-expanding valves but only 3 patients received a mechanical-expanding valve. Acknowledging these limitations, the findings unveil that specific anatomic factors may play a role in the occurrence of PVL as well.

This may not be surprising considering the anatomy of the base of the heart and its functional consequences. The LCC is located upstream of the so-called aortic-mitral continuity curtain.[23][24] At the level of the "annulus," the LCC juxtaposes the ventricular mass and left fibrous trigone (LFT) on one side and the NCC on the other and is separated from

https://doi.org/10.4250/jcvi.2021.0141

Journal of Cardiovascular Imaging JCVI

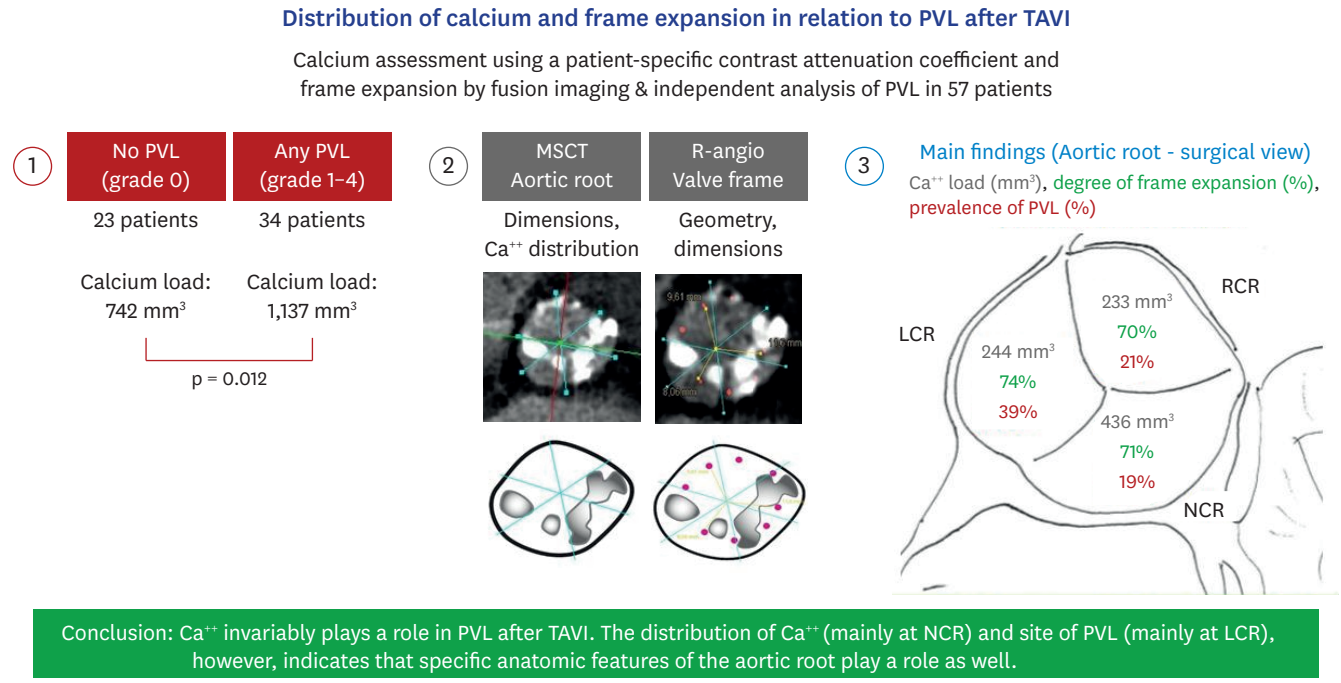

Figure 3. Central illustration. Overview of methodology and main findings.
LCR: left coronary cusp region, MSCT: multislice computed tomography, NCR: non coronary cusp region, PVL: paravalvular leakage, R-angio: rotational angiography, TAVI: transcatheter aortic valve implantation.

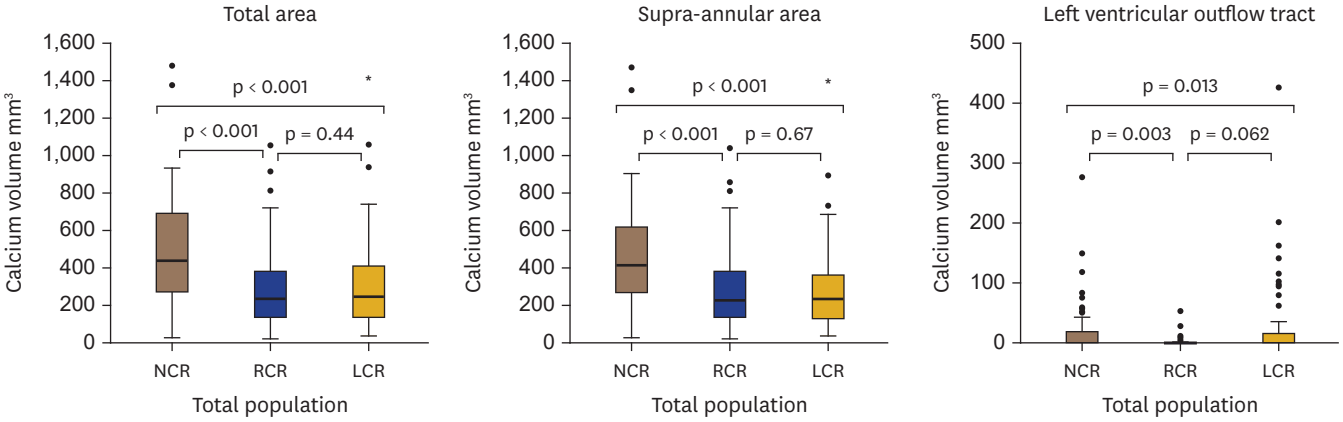

Figure 4. Comparison of the calcium volume between the different areas and the different coronary region. Boxplots including median (horizontal line within box) as well as 25th to 75th percentiles.
LCR: left coronary cusp region, NCR: non coronary cusp region, RCR: right coronary cusp region.

Table 3. Results of the logistic regression using generalized estimating equations for association with paravalvular leakage

Univariate analysis	OR (95% CI)	p-value
Location		
Non coronary cusp	Reference	
Right coronary cusp	1.12 (0.46–2.69)	0.810
Left coronary cusp	2.63 (1.12–6.19)	0.027
Determinants		
Calcium load aortic root (mm³)/1,000	4.83 (1.66–14.09)	0.004
Calcium load SAA (mm³)/1,000	4.75 (1.52–14.88)	0.007
Calcium load LVOT (> 100 mm³)	2.36 (0.56–9.91)	0.240
Degree of expansion at the annulus (%)	0.99 (0.96–1.01)	0.290

OR: odds ratio, CI: confidence interval, SAA: supra-annular area, LVOT: left ventricular outflow tract.

https://doi.org/10.4250/jcvi.2021.0141

Journal of Cardiovascular Imaging JCVI

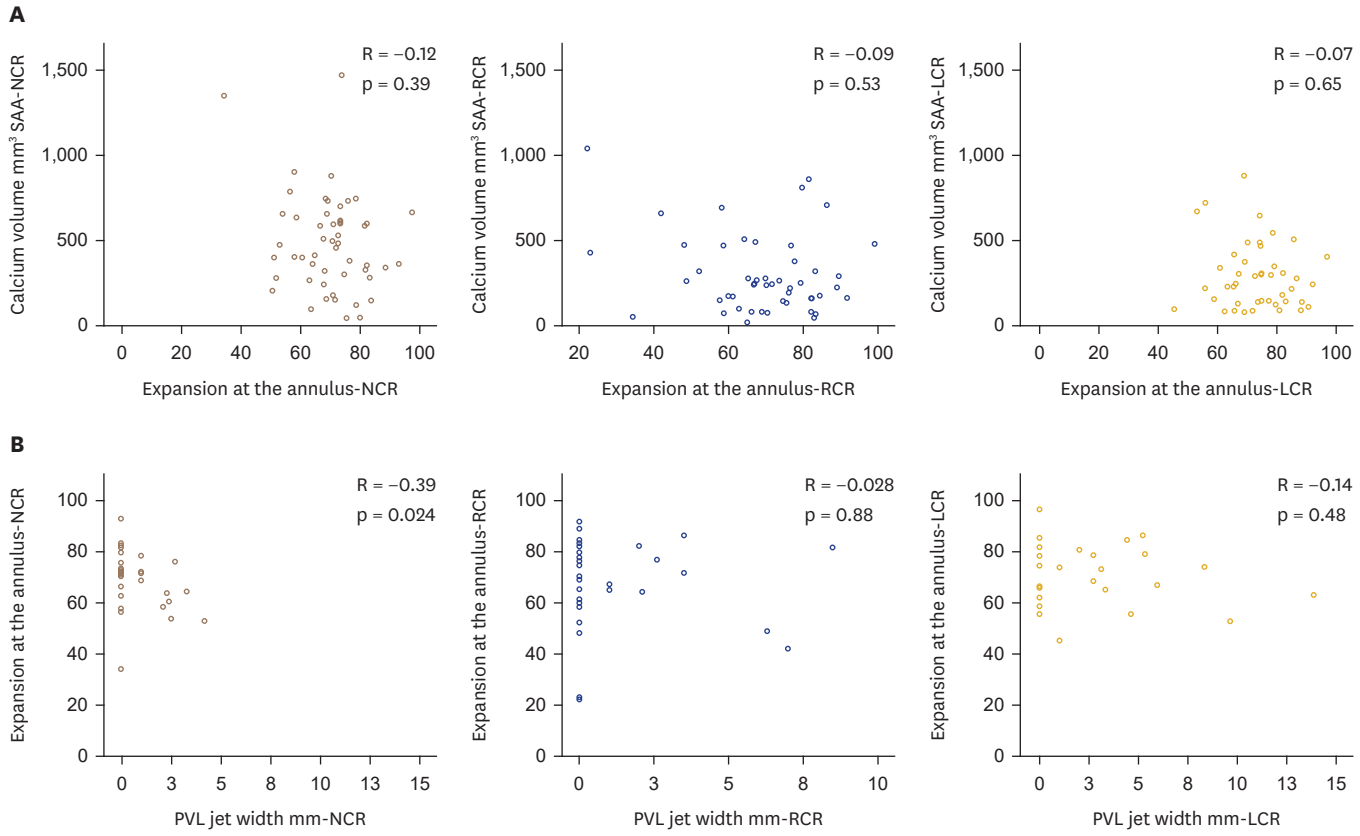

Figure 5. (A) Spearman-Rho correlation coefficient to assess the relation between degree of frame expansion and calcium load in the entire cohort and (B) to assess the relation between degree of frame expansion and PVL jet width in patients with PVL.
LCR: left coronary cusp region, NCR: non coronary cusp region, PVL: paravalvular leakage, RCR: right coronary cusp region.

the latter by an interleaflet triangle. The aortic-mitral curtain is reinforced to either side by the thick dense fibrous tissue of the LFT and right fibrous trigone (RFT) at, respectively, the nadir of the LCC and NCC. This area of fibrous continuity between the LFT and RFT provides the support for the anterior mitral leaflet.[25] The area occupied by the interleaflet triangle between the right coronary cusp (RCC) and NCC, membranous septum below those 2 cusps and the RFT (the latter 2 being the main constituents of the central fibrous body), separates the RCC from the aortic-mitral curtain. While long considered a static structure, the aortic-mitral curtain varies in size during the cardiac cycle.[26] Similar to other studies, we found that most calcium was located at the NCR but at the level of the LVOT, most calcium was below the LCR.[18][27] These findings support the concept that calcification of the base of the root progresses "downwards" into the aortic-mitral curtain.[28][29]

From a methodological point of view, calcium quantification was performed using a patient specific calcium detection threshold proposed by Hansson et al.[18] This is in contrast with previous studies so far reported that provided only qualitative or semi-quantitative information.

As it concerns a mechanics study, no distinction in severity of PVL was made. We acknowledge the complexity and pitfalls of the assessment of the presence and severity of PVL by TTE, necessitating a multi-parametric approach. In this study, the presence and severity of PVL was based on a standard core lab analysis plan (VARC-2 adapted), which mainly focused on the detection of PVL in the PSAX view combined with 3 long-axis views

https://doi.org/10.4250/jcvi.2021.0141

using colour Doppler. The location of PVL was assessed mainly in the PSAX view using a clock model complemented with 3 long-axis views. It is believed that the multiple-view approach demonstrates a comprehensive evaluation around the circumference of the valve frame that may reduce the rate of false negative findings when using only the PSAX view.[22] As the circumferential extent of PVL in the PSAX view can over- and underestimate PVL, quantification of PVL in this study was based upon the measurement of the mosaic jet radial width, thereby, avoiding miscalculation a wide spread PVL along the valve frame with a small radial width or the inverse.[22] Additionally, the jet radial width is argued to be the most accurate parameter in assessing PVL and the only quantitative parameter that could be measured in all views in contrast with jet area, which can only be measured in the PSAX view and may suffer from false negative findings.[22] More importantly, since we used a quantitative measure to define the calcium load, we felt that a quantitative measure of PVL (jet width) is more appropriate than a semi-quantitative grading of PVL.

Fusion imaging that we used in this study is based upon the integration of the patient's baseline aortic root anatomy from the pre-procedural CT with the frame morphology after valve deployment that was derived from the post-procedural R-angio while respecting procedural details such as X-ray working view, orientation of aortic root, depth of implantation etc. It is similar to the work done by Ruile et al.[30] who also demonstrated the feasibility of fusing imaging based upon pre- and post TAVI CT in 120 patients for the evaluation of valve position relative to the aortic annulus. The clinical application of R-angio as a tool has been demonstrated in earlier studies.[8][9][19][20] Further research is needed to prove the clinical value of the current concept of fusion imaging.

In conclusion, in patients referred for TAVI, aortic root calcium is predominantly located at the NCR and was independently associated with PVL. No other patient- and/or procedure-related factors were found. The site of PVL was, however, predominantly at the LCR. These findings indicate that in addition to calcium, specific anatomic features likely play a role in the occurrence of PVL after TAVI.

SUPPLEMENTARY MATERIALS

Supplementary Table 1
Reproducibility of calcium scoring

Click here to view

Supplementary Figure 1
Echo Doppler paravalvular leakage assessment.

Click here to view

REFERENCES

1. Smith CR, Leon MB, Mack MJ, et al. Transcatheter versus surgical aortic-valve replacement in high-risk patients. *N Engl J Med* 2011;364:2187-98.
PUBMED | CROSSREF

2. Leon MB, Smith CR, Mack MJ, et al. Transcatheter or surgical aortic-valve replacement in intermediate-risk patients. *N Engl J Med* 2016;374:1609-20.
PUBMED | CROSSREF

3. Reardon MJ, Van Mieghem NM, Popma JJ, et al. Surgical or transcatheter aortic-valve replacement in intermediate-risk patients. *N Engl J Med* 2017;376:1321-31.
PUBMED | CROSSREF

4. Popma JJ, Deeb GM, Yakubov SJ, et al. Transcatheter aortic-valve replacement with a self-expanding valve in low-risk patients. *N Engl J Med* 2019;380:1706-15.
PUBMED | CROSSREF

5. Mack MJ, Leon MB, Thourani VH, et al. Transcatheter aortic-valve replacement with a balloon-expandable valve in low-risk patients. *N Engl J Med* 2019;380:1695-705.
PUBMED | CROSSREF

6. Padang R, Ali M, Greason KL, et al. Comparative survival and role of STS score in aortic paravalvular leak after SAVR or TAVR: a retrospective study from the USA. *BMJ Open* 2018;8:e022437.
PUBMED | CROSSREF

7. Abdel-Wahab M, Mehilli J, Frerker C, et al. Comparison of balloon-expandable vs self-expandable valves in patients undergoing transcatheter aortic valve replacement: the CHOICE randomized clinical trial. *JAMA* 2014;311:1503-14.
PUBMED | CROSSREF

8. Rodríguez-Olivares R, Rahhab Z, Faquir NE, et al. Differences in frame geometry between balloon-expandable and self-expanding transcatheter heart valves and association with aortic regurgitation. *Rev Esp Cardiol (Engl Ed)* 2016;69:392-400.
PUBMED | CROSSREF

9. Rodríguez-Olivares R, El Faquir N, Rahhab Z, et al. Does frame geometry play a role in aortic regurgitation after Medtronic CoreValve implantation? *EuroIntervention* 2016;12:519-25.
PUBMED | CROSSREF

10. Di Martino LF, Soliman OI, van Gils L, et al. Relation between calcium burden, echocardiographic stent frame eccentricity and paravalvular leakage after corevalve transcatheter aortic valve implantation. *Eur Heart J Cardiovasc Imaging* 2017;18:648-53.
PUBMED | CROSSREF

11. Rahhab Z, El Faquir N, Rodríguez-Olivares R, et al. Determinants of aortic regurgitation after transcatheter aortic valve implantation. An observational study using multi-slice computed tomography-guided sizing. *J Cardiovasc Surg (Torino)* 2017;58:598-605.
PUBMED | CROSSREF

12. Abdelghani M, Mankerious N, Allali A, et al. Bioprosthetic valve performance after transcatheter aortic valve replacement with self-expanding versus balloon-expandable valves in large versus small aortic valve annuli: insights from the CHOICE trial and the CHOICE-Extend registry. *JACC Cardiovasc Interv* 2018;11:2507-18.
PUBMED | CROSSREF

13. Rodríguez-Olivares R, El Faquir N, Rahhab Z, et al. Impact of device-host interaction on paravalvular aortic regurgitation with different transcatheter heart valves. *Cardiovasc Revasc Med* 2019;20:126-32.
PUBMED | CROSSREF

14. Haensig M, Lehmkuhl L, Rastan AJ, et al. Aortic valve calcium scoring is a predictor of significant paravalvular aortic insufficiency in transapical-aortic valve implantation. *Eur J Cardiothorac Surg* 2012;41:1234-41.
PUBMED | CROSSREF

15. Achenbach S, Delgado V, Hausleiter J, Schoenhagen P, Min JK, Leipsic JA. SCCT expert consensus document on computed tomography imaging before transcatheter aortic valve implantation (TAVI)/transcatheter aortic valve replacement (TAVR). *J Cardiovasc Comput Tomogr* 2012;6:366-80.
PUBMED | CROSSREF

16. Ewe SH, Ng AC, Schuijf JD, et al. Location and severity of aortic valve calcium and implications for aortic regurgitation after transcatheter aortic valve implantation. *Am J Cardiol* 2011;108:1470-7.
PUBMED | CROSSREF

17. Schultz C, Moelker A, Tzikas A, et al. The use of MSCT for the evaluation of the aortic root before transcutaneous aortic valve implantation: the Rotterdam approach. *EuroIntervention* 2010;6:505-11.
PUBMED | CROSSREF

18. Hansson NC, Nørgaard BL, Barbanti M, et al. The impact of calcium volume and distribution in aortic root injury related to balloon-expandable transcatheter aortic valve replacement. *J Cardiovasc Comput Tomogr* 2015;9:382-92.
PUBMED | CROSSREF

19. Rodríguez-Olivares R, El Faquir N, Rahhab Z, et al. Determinants of image quality of rotational angiography for on-line assessment of frame geometry after transcatheter aortic valve implantation. *Int J Cardiovasc Imaging* 2016;32:1021-9.
PUBMED | CROSSREF

20. Schultz CJ, Lauritsch G, Van Mieghem N, et al. Rotational angiography with motion compensation: first-in-man use for the 3D evaluation of transcatheter valve prostheses. *EuroIntervention* 2015;11:442-9.
PUBMED | CROSSREF

21. Kappetein AP, Head SJ, Généreux P, et al. Updated standardized endpoint definitions for transcatheter aortic valve implantation: the Valve Academic Research Consortium-2 consensus document. *J Am Coll Cardiol* 2012;60:1438-54.
PUBMED | CROSSREF

22. Pibarot P, Hahn RT, Weissman NJ, Monaghan MJ. Assessment of paravalvular regurgitation following TAVR: a proposal of unifying grading scheme. *JACC Cardiovasc Imaging* 2015;8:340-60.
PUBMED | CROSSREF

23. McAlpine WA. The branches of the coronary arteries. In: Heart and Coronary Arteries: An Anatomical Atlas for Clinical Diagnosis, Radiological Investigation, and Surgical Treatment. New York, NY: Springer-Verlag; 1975. p.163–78.

24. Piazza N, de Jaegere P, Schultz C, Becker AE, Serruys PW, Anderson RH. Anatomy of the aortic valvar complex and its implications for transcatheter implantation of the aortic valve. *Circ Cardiovasc Interv* 2008;1:74-81.
PUBMED | CROSSREF

25. Muresian H. The clinical anatomy of the mitral valve. *Clin Anat* 2009;22:85-98.
PUBMED | CROSSREF

26. Parish LM, Jackson BM, Enomoto Y, Gorman RC, Gorman JH 3rd. The dynamic anterior mitral annulus. *Ann Thorac Surg* 2004;78:1248-55.
PUBMED | CROSSREF

27. Fujita B, Kütting M, Seiffert M, et al. Calcium distribution patterns of the aortic valve as a risk factor for the need of permanent pacemaker implantation after transcatheter aortic valve implantation. *Eur Heart J Cardiovasc Imaging* 2016;17:1385-93.
PUBMED | CROSSREF

28. Desai MY, Wu W, Masri A, et al. Increased aorto-mitral curtain thickness independently predicts mortality in patients with radiation-associated cardiac disease undergoing cardiac surgery. *Ann Thorac Surg* 2014;97:1348-55.
PUBMED | CROSSREF

29. van der Boon RM, Nuis RJ, Van Mieghem NM, et al. New conduction abnormalities after TAVI--frequency and causes. *Nat Rev Cardiol* 2012;9:454-63.
PUBMED | CROSSREF

30. Ruile P, Pache G, Minners J, Hein M, Neumann FJ, Breitbart P. Fusion imaging of pre- and post-procedural computed tomography angiography in transcatheter aortic valve implantation patients: evaluation of prosthesis position and its influence on new conduction disturbances. *Eur Heart J Cardiovasc Imaging* 2019;20:781-8.
PUBMED | CROSSREF